

*Araştırma Makalesi – Research Article*

## Finite Element Modelling of Ultimate Strength of CFST Column and Its Comparison with Design Codes

### BDÇT Kolonların Nihai Dayanımının Sonlu Elemanlar ile Modellenmesi ve Tasarım Kodları ile Karşılaştırılması

Ayşegül Erdoğan<sup>1</sup>, Esra Mete Güneysisi<sup>2</sup>, Süleyman İpek<sup>3\*</sup>

*Geliş / Received: 07/12/2021*

*Revize / Revised: 25/04/2022*

*Kabul / Accepted: 25/04/2022*

#### ABSTRACT

Concrete-filled steel tube (CFST) members have high strength, stiffness, and ductility properties, which makes them favorable in structural applications. This study purposes to create a finite element analysis-based model for designing the peak strength of axially loaded CFSTcircular columns. To this aim, 314 test specimens presented in the previous experimental studies were investigated. In the study, the wall thickness and yield strength of steel tube, compressive strength of concrete, and column diameter and length were designated as the design parameters. In this regard, the design model created using the finite element analysis proposed in this study was evaluated comparatively with existing ones given in the existing design codes and standards such as ACI, AS, AISC, AIJ, Eurocode 4, DL/T, and CISC. Besides, the estimation performance of all design models was examined statistically as well.

**Keywords-***Axial Loading, CFST Columns, Experimental Database, Finite Element Analysis, Ultimate Strength*

#### ÖZ

Beton dolgulu çelik tüpler (BDÇT), yüksek mukavemet, rijitlik ve süneklik özelliklerine sahiptir, bu da onları yapısal uygulamalarda avantajlı kılmaktadır. Bu çalışma, aksel yüke maruz beton dolgulu çelik tüp şeklindeki dairesel kolonların nihai dayanımını tasarlamak için bir sonlu elemanlar analiz modeli oluşturmayı amaçlamaktadır. Bu amaçla, daha önceki deneysel çalışmalarda sunulan 314 test numunesi incelenmiştir. Çalışmada, çelik boru et kalınlığı ve akma dayanımı, beton basınç dayanımı ve kolon çapı ve uzunluğu tasarım parametreleri olarak belirlenmiştir. Bu bağlamda, bu çalışmada önerilen sonlu elemanlaryöntemi kullanılarak oluşturulan tasarım modeli, ACI, AS, AISC, AIJ, Eurocode 4, DL/T ve CISC gibi mevcut tasarım kodlarında verilen mevcut tasarım modelleri ile karşılaştırmalı olarak değerlendirilmiştir. Ayrıca tüm tasarım modellerin tahmin performansı da istatistiksel olarak incelenmiştir.

**Anahtar Kelimeler-***Eksenel Yükleme, BDÇT Kolonlar, Deneysel Veri Tabanı, Sonlu Elemanlar Analizi, Nihai Dayanım*

<sup>1</sup>Contact: [aygl1988@hotmail.com](mailto:aygl1988@hotmail.com) (<https://orcid.org/0000-0001-8192-4675>)

*Civil Engineering Department, Engineering Faculty, Gaziantep University, Gaziantep, Turkey*

<sup>2</sup>Contact: [eguneyisi@gantep.edu.tr](mailto:eguneyisi@gantep.edu.tr) (<https://orcid.org/0000-0002-4598-5582>)

*Civil Engineering Department, Engineering Faculty, Gaziantep University, Gaziantep, Turkey*

<sup>3\*</sup>Corresponding author contact: [sipek@bingol.edu.tr](mailto:sipek@bingol.edu.tr) (<https://orcid.org/0000-0001-8891-949X>)

*Department of Architecture, Faculty of Engineering and Architecture, Bingöl University, Bingöl, Turkey*

## I. INTRODUCTION

CFST members have been widely employed in modern buildings, bridges, sports stadia, towers, and offshore structures due to including high strength, stiffness, and ductility characteristics [1-3]. The ductility and strength characteristics of the CFST columns subjected to compression load are improved thanks to the efficient confinement provided to the concrete infill by the encircling steel tube. Furthermore, the presence of the infill concrete aids in the enhancement of the steel tube's local buckling response and the prevention of inward buckling. Besides, the steel tube plays a formwork role during the construction, and thus, a more economical and faster construction process is achieved [4,5]. Therefore, it can be stated that the construction of the CFST columns saves time, as the steel tube serves as a permanent formwork [6].

Many studies, both experimental and analytical, have been carried out to examine the properties, practices, and behavior of the CFST elements [7-13]. Surveying the available literature, it has been found that the steel tube with a concrete core had almost 49% higher flexural strength capacity than the steel tube without a concrete core [14]. The studies available in the literature cover the examination of the influences of three critical issues such as the thickness of the steel tube, the bond strength occurring between the concrete core and encircling steel tube, as well as the confinement provided by the steel tube, on the characteristics and behavior of the axially loaded CFST circular columns involving a broad array of concrete strengths. The experimental results were compared to the design specifications' predictions [15]. Designating the ultimate bearing capacity of axially loaded CFST columns by experimental studies has become an important studying field for researchers. For this reason, it can be expressed that the experimental studies of CFST columns have become a popular subject for engineering studies and applications.

Finite element analysis (FEA), which is an extensively used numerical approach for performing various engineering analyses in the literature, is based on the finite element method (FEM) that provides solutions by simplifying complex engineering problems. Furthermore, with greater computer effort, the approximation computations in the FEM can be enhanced or adjusted [16]. In the literature, there are several studies, in which the FEM has been successfully used to investigate the behavior and characteristics of CFST members [17-22]. For instance, Wang et al. [20] presented a study in which the impact performance of CFST elements was investigated. They obtained the time history and failure modes of the impact forces for the composite elements under the lateral impact. An FEA model has been created to examine the effects of the strain rate for concrete and steel materials and the interaction occurring between the steel tube and concrete core. In addition, the effect of steel tube confinement has been taken into account. Dataset was used to confirm the reliability of the FEA model, and in general, compatible results were obtained. Ellobody et al. [22] presented a nonlinear finite element technique-based analysis of normal and high-strength CFST circular stub columns. Also, a parametric study was conducted to evaluate the influence of various concrete strengths as infill material. However, it should be emphasized that more studies are required to better understand the structural response of such composite columns.

In this context, this study aims to create an FEA model for determining the ultimate load-carrying capacity ( $N_u$ ) of CFST circular columns. To this, a FEM-based program named ABAQUS [23] was employed to construct the FEM model. A total of 314 experimental data specimens compiled from previously conducted studies available in the literature were utilized to evaluate the performance of the FEM model. The design parameters were listed as the column diameter (D), wall thickness (t) and yield strength ( $f_y$ ) of steel tube, concrete compressive strength ( $f_c$ ), and column length (L). As a result, the design model developed using the FEM was compared with the design models proposed by the codes and standards [24-32]. Moreover, the performance of the FEM model and the other ones were evaluated in terms of statistical parameters.

## II. EXISTING FORMULATIONS IN DESIGN CODES

The formulations specified in the design codes are summarized here. The American Concrete Institute [24] and Australian Standards [25-26] have proposed the same formula, which was labeled as ACI/AS in the current study, for estimating the ultimate axial load carrying capacity of the CFST circular columns. The ACI/AS equation disregards the confinement effect and is expressed as in Equation 1:

$$N_u = 0.85f'_c A_c + f_y A_s \quad (1)$$

where

$f'_c$  is the concrete compressive strength measured on standard cylinders

$A_c$  is the cross – sectional area of concrete core

$f_y$  is the yield strength of steel tube

$A_s$  is the cross – sectional area of steel tube

However, the expression proposed in the American Institute of Steel Construction (AISC) [27] contains the confinement effect presented as follows:

In the case of  $P_e \geq 0.44P_{0,AISC}$ ,

$$N_u = P_{0,AISC} \left[ 0.658 \left( \frac{P_{0,AISC}}{P_e} \right) \right] \quad (2)$$

in which the nominal strength ( $P_{0,AISC}$ ) and elastic buckling load ( $P_e$ ) is expressed as follows:

$$P_{0,AISC} = 0.95f'_c A_c + f_y A_s \quad (3)$$

$$P_e = \frac{\pi^2(EI)_{eff1}}{(K_A L_A)^2} \quad (4)$$

where

$K_A$  is the effective length factor

$L_A$  is the laterally unbraced length of the column

The equation of the effective stiffness of the composite section  $(EI)_{eff1}$  in the elastic buckling load ( $P_e$ ) is given as follows:

$$(EI)_{eff1} = E_s I_s + C_3 E_{c1} I_c \quad (5)$$

where

$E_s$  is the modulus of elasticity of steel

$I_s$  is the moment of inertia of steel tube

$E_{c1}$  is the modulus of elasticity of concrete ( $4730x\sqrt{f'_c}$  in MPa) (for the normal weight concrete)

$I_c$  is the moment of inertia of concrete core

The expression of the coefficient  $C_3$  stated in Equation 5 is presented in Equation 6 as follows:

$$C_3 = 0.6 + 2 \left( \frac{A_s}{A_c + A_s} \right) \leq 0.9 \quad (6)$$

The formulation suggested by the Architectural Institute of Japan (AIJ) [28-29] comprises the confinement factor ( $\eta$ ) for effective length-to-diameter ( $l_k/D$ ) greater than 4. The confinement factor ( $\eta$ ) enhances the load-carrying capacity owing to the interaction occurring between the steel tube and concrete core. The formulation proposed by AIJ is expressed as in Equation 7:

$$N_u = 0.85f'_c A_c + (1.0 + \eta)f_y A_s \quad (7)$$

In order to estimate the load-carrying capacity of CFST columns, Eurocode 4 [30] proposed expressions that consider both the confinement effect and the contribution depending on the steel tube and concrete interaction. These expressions are presented as follows:

$$N_u = \left( 1 + \eta_c \frac{t}{D} \frac{f_y}{f'_c} \right) f'_c A_c + \eta_a f_y A_s \quad (8)$$

where

$\eta_c$  is the confinement coefficient for the concrete

$\eta_a$  is the confinement coefficient for the steel tube

These coefficients are expressed as follows:

$$\eta_c = 4.9 - 18.5\bar{\lambda} + 17\bar{\lambda}^2 (\eta_c \geq 0) \quad (9)$$

$$\eta_a = 0.25(3 + 2\bar{\lambda}) (\eta_a \leq 1.0) \quad (10)$$

in which the relative slenderness ( $\bar{\lambda}$ ) is expressed as follows:

$$\bar{\lambda} = \sqrt{\frac{N_{pIR}}{N_{cr}}} \quad (11)$$

in which the equations for  $N_{pIR}$  and  $N_{cr}$  given in Equation 11 are expressed as follows:

$$N_{pIR} = f_y A_s + f'_c A_c \quad (12)$$

$$N_{cr} = \frac{\pi^2 (EI)_{eff2}}{l^2} \quad (13)$$

in which the equation for the effective flexural stiffness  $(EI)_{eff2}$  given in Equation 13 is presented as follows:

$$(EI)_{eff2} = E_s I_s + K_e E_{c2} I_c \quad (14)$$

where  $K_e$  and  $E_{c2}$  are the correction factor (0.6) and the elastic modulus of concrete (expressed as  $E_{c2} = 22000[(f'_c + 8)/10]^{0.3}$  in MPa), respectively. However, when the relative slenderness ( $\bar{\lambda}$ ) is equal to 0, the sectional capacity ( $P_{0,EC4}$ ) can be determined using the expression given below:

$$P_{0,EC4} = \left(1 + 4.9 \frac{t}{D} \frac{f_y}{f'_c}\right) f'_c A_c + 0.75 f_y A_s \quad (15)$$

The expression in Chinese code (DL/T) [31] assumes that a CFST stub column consists of a single material that has a nominal yield strength of the composite section ( $f_{scy}$ ). This expression is presented as follows:

$$N_u = f_{scy} (A_s + A_c) \quad (16)$$

$$f_{scy} = (1.212 + B\xi + C\xi^2) f_{ck} \quad (17)$$

in which the coefficients  $B$  and  $C$ , the confinement factor ( $\xi$ ), and  $f_{ck}$  are presented as follows:

$$B = 0.1759 \frac{f_y}{235} + 0.974 \quad (18)$$

$$C = -0.1038 \frac{f_{ck}}{20} + 0.0309 \quad (19)$$

$$\xi = \frac{A_s f_y}{A_c f_{ck}} \quad (20)$$

$$f_{ck} = 0.67 f_{cu} \quad (21)$$

where

$f_{ck}$  is the characteristic concrete strength

$f_{cu}$  is the 150 – mm cubic concrete compressive strength

Finally, the Canadian Institute of Steel Construction (CISC) [32] has proposed an equation, which involves some material and geometric properties, expressed as follows:

$$N_u = \tau N_r + \tau' N'_r \quad (22)$$

$$N_r = \phi A_s f_y (1 + \lambda^{2n})^{-\frac{1}{n}} \quad (23)$$

$$\lambda = \frac{KL}{r_s} \sqrt{\frac{f_y}{\pi^2 E_s}} \quad (24)$$

$$N'_r = 0.85 \phi_c f'_c A_c \lambda_c^{-2} [\sqrt{1 + 0.25 \lambda_c^{-4}} - 0.5 \lambda_c^{-2}] \quad (25)$$

where

$\phi$  is the resistance factor

$n$  is the number of data samples

$r_s$  is the radius of gyration of steel

$\phi_c$  is the coefficient, equal to 0.6

The expression of  $\lambda_c$  given in Equation 25 is presented as follows:

$$\lambda_c = \frac{KL}{r_c} \sqrt{\frac{f'_c}{\pi^2 E_c}} \quad (26)$$

where

$r_c$  is the radius of the gyration of concrete

The formulations of  $\tau$  and  $\tau'$  are expressed as follows:

$$\tau = \frac{1}{\sqrt{1+\rho+\rho^2}} \quad (27)$$

$$\tau' = 1 + \left(\frac{25\rho^2\tau}{(D/t)}\right) \left(\frac{f_y}{0.85f'_c}\right) \quad (28)$$

$$\rho = 0.02(25 - L/D) \quad (29)$$

### III. FINITE ELEMENT MODELING

To accurately examine the nonlinear behavior of the axially loaded CFST columns, the three fundamental parameters of such composite members should be first described and modeled. These fundamental parameters are the characteristics of steel tube and concrete core, and the interface occurring between the steel tube and concrete core. In this respect, the steel tube and its endplates have been described as bilinear isotropic hardening with elastic-plastic material behavior. In the study of Han and Huo [33], the stress-strain curve for steel has comprised of two parts, namely elastic and plastic zones. As can be seen in Figure 1a, the elastic properties of steel have been defined in the first part, from the origin point to the yield point of steel while the plastic region has been utilized in characterizing the elastic modulus. In this regard, the behavior of steel in ABAQUS [23] has been defined as elastic in the first region that is up to the yield strain, and plastic in the second region between the yield and final strain.

In another respect, based on the studies of Hu et al. [34] and Binici [35], the concrete has been modeled with a stress-strain characteristic consisting of three regions, see Figure 1b. The elastic zone, which is the first zone of this characteristic, covers a region starting from the origin point and ending at the proportional limit stress. On the other hand, the second part of the stress-strain characteristic of concrete is a nonlinear zone that is between the confined concrete stress and proportional limit. The zone starting from the confined concrete stress and extending along to the final strength value of the curve forms the third part of the stress-strain relation of the concrete core. In order for detailed calculations of stress-strain relationships of steel tube and concrete materials, see the study carried out by İpek et al. [36].

The deformable solid has been used to describe and model the steel tube and concrete, while the discrete rigid has been designated to model the endplates. The steel tube and concrete components have been designed by choosing the reduced integration and geometric order of linear, namely C3D8, which has a triangle element shape. Besides, the endplates have been modeled as the geometric order of linear, namely R3D3, which has a hexahedron element type.

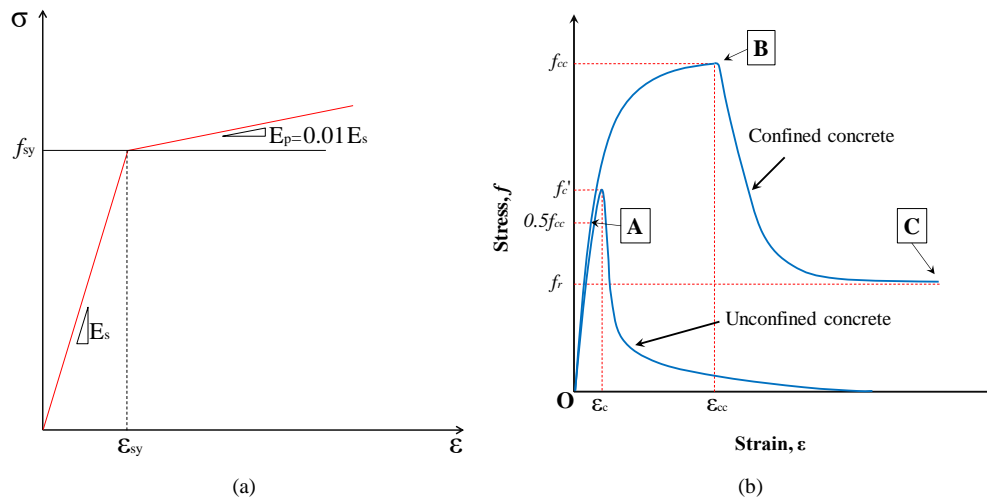


**Figure 1.** Stress-strain behavior of (a) steel end plates and tubes [33] and (b) confined and unconfined concrete [34-36]

On the top and bottom endplates, a reference (RF) point has been composed to constitute a rigid body constraint and to determine their center. The boundary conditions and loadings have been defined from these RF points of the models. The bottom endplates have been modeled as fixed support against all degrees of freedom. Nevertheless, the top plate on which the load is applied has been released in the direction of loading. The RF point of the top endplate has been loaded as the static uniform loading by specified displacement. However, the boundary condition at the bottom has been fixed against 4 degrees of freedom ( $u_x = u_y = u_z = \theta_z = 0$ ). Namely, the bottom plate of the model has been only allowed to rotate about x and y axes. On the other hand, the top plate was allowed to deform in the z-direction and rotate about the x and y axes. In other words, deformations in the x and y directions in the top plate and rotation around the z-axis have not been allowed ( $u_x = u_y = \theta_z = 0$ ).

#### IV. VERIFICATION OF FEM DESIGN MODEL

Both the calibration and verification of such models are very important to properly predict the response and characteristics of such columns. Apart from estimating the ultimate axial strength, the load-displacement curves obtained from the developed FEM design model for the CFST circular columns have been also examined to evaluate the estimation performance of the design model. Figures 2a and 2b demonstrate the axial load-displacement relationships of the D4M3C and D4M4C samples taken from the experimental study carried out by Gupta et al. [17] and their comparison with those obtained from the FEM design model developed in this study. The D4M3C and D4M4C named CFST column specimens had the same outer steel tube diameter and steel tube thickness of 112.56 mm and 2.89 mm, respectively. Both column specimens had the same height and steel tube yield strength of 340 mm and 360 MPa, respectively. The only difference between these two column specimens was the concrete grade. The D4M3C named column specimen was manufactured with concrete having 30 MPa compressive strength while the D4M4C named one was produced with concrete having 40 MPa compressive strength. The experimental results revealed that the concrete compressive strength has an effect on both the load-carrying capacity and ductility performance of such columns. The CFST column specimen manufactured with a higher concrete compressive strength yielded more ductile behavior. It can be also seen that the concrete compressive strength does not significantly influence the behavior of such columns after peak strength (in the strain-softening region). Almost similar observations were achieved from the developed FEM design model. Increasing the compressive strength led to an increase in the load-carrying capacity without affecting the post-peak performance.

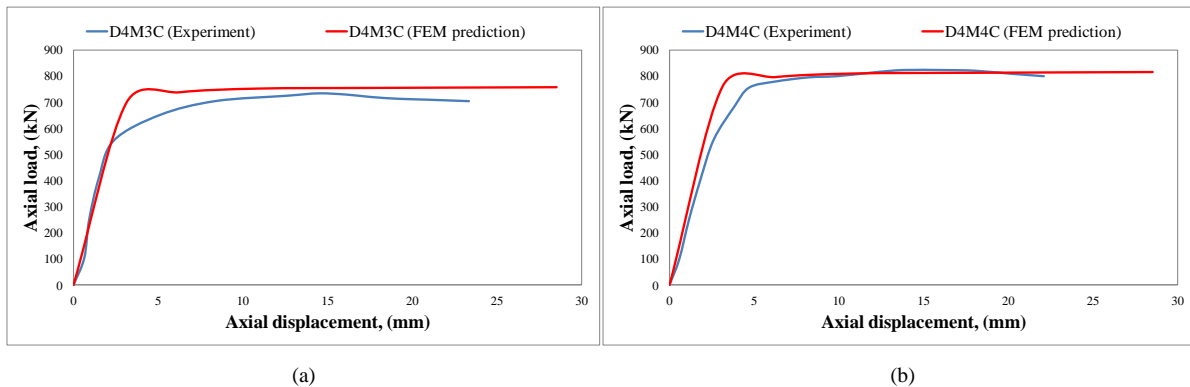


**Figure 2.** Axial load vs. displacement of: (a) D4M3C and (b) D4M4C specimens in the study of Gupta et al. [17] and those predicted by FEM

In addition, minor variations between the experimental and predicted load versus strain (displacement) curves obtained in the current study are thought to be the result of a discrepancy in the component and interaction models. It should be noted that discrepancies in the actual and predicted load versus displacement curves resulted from a failure to simulate the true circumstances, which included material strengths, boundary conditions, testing equipment accuracy, starting flaws, and manufacturing faults. Furthermore, it should be noted that a complete simulation of all real-world testing conditions in finite element analysis is not feasible, and that concrete features cannot be defined just by strength tests, even if the concrete strength is determined on the day of the column's testing. As a result, it may be inferred that such disparities between real-world test conditions and finite element analysis cannot be eliminated.

Similarly, Figures 3a and 3b show the comparison of the experimental axial load vs. strain curves of the column specimens CU-070 and CU-150 given in the study of Huang et al. [37] with the graph obtained from the FEM prediction. The CU-070 named CFST circular column had an outer diameter of 280 mm and a tube thickness of 4 mm while the CU-150 named CFST circular column had an outer diameter of 300 mm and a tube thickness of 2 mm. Thereby, the diameter-to-thickness ratio of the CU-070 named column was 70 and that of the CU-150 named was 150. Besides, the yield strengths of steel tubes of these specimens were, respectively, 272.6 MPa and 341.7 MPa whereas their concrete cube strengths were 31.2 MPa and 27.2 MP, respectively. As can be seen from the figures, increasing the diameter-to-thickness ratio resulted in lower ultimate axial strength and caused a sudden decrease in the load-bearing capacity after the peak strength. A similar diameter-to-thickness ratio-dependent decrease in the ultimate axial strength was observed in the results of the developed FEM model; however, the sudden reduction in the strain-softening region was not achieved in the model.

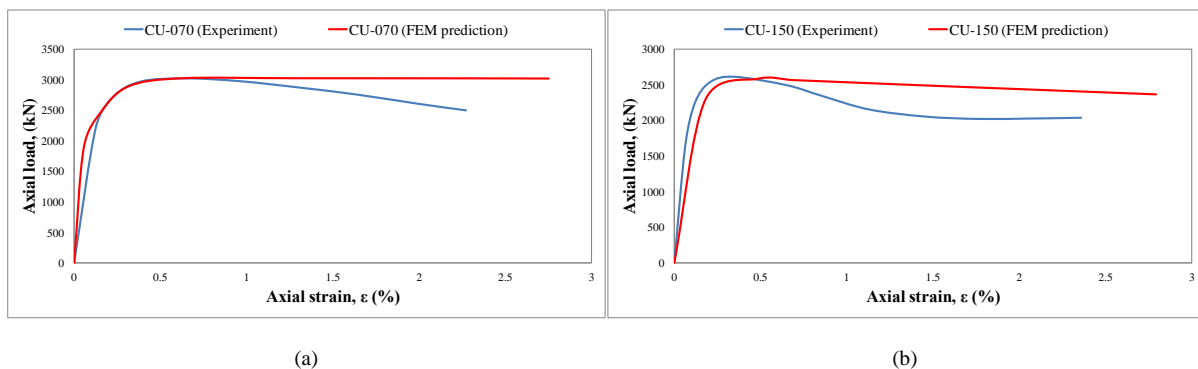


**Figure 3.** Axial load vs. axial strain of: (a) CU-070 and (b) CU-150 specimens in the study of Huang et al. [37] and those predicted by FEM

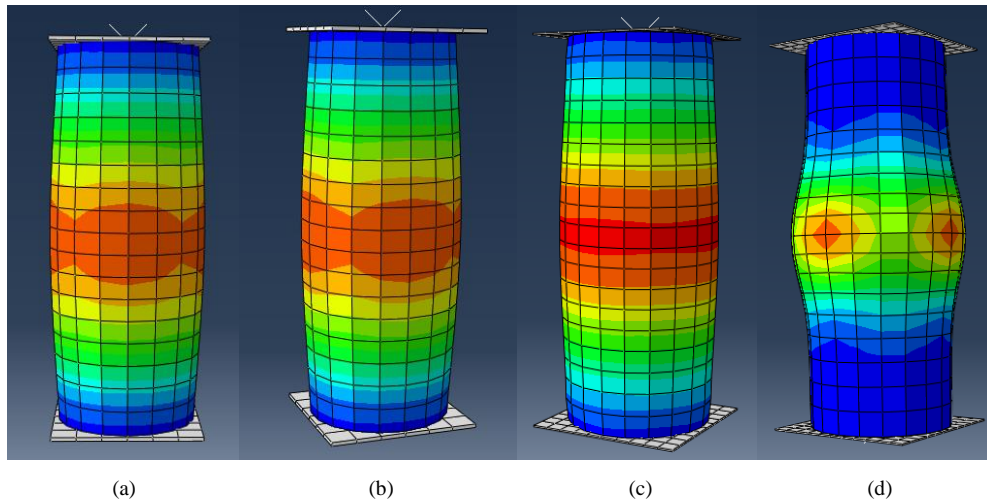


**Figure 4.** Simulated deformed shapes of the CFST circular column specimens labeled:(a) D4M3C and (b) D4M4C [17] and (c) CU-070 and (d) CU-150 [37] (from FEM analysis)

In the aforementioned studies, the deformed shapes of the CFST circular column specimens labeled D4M3C and D4M4C [17] and CU-070 and CU-150 [37] were not provided. However, in general, the failure modes of the sample vary depending on the steel tube yielding strength and thickness, the concrete compressive strength, the column slenderness, and the confinement effect (namely, interaction between the steel tube and concrete). , the FEA performed on the ABAQUS Software provided the simulated deformed shapes of these specimens. When the simulated deformed shapes of specimens were investigated, it would be seen that these specimens tend to have bulged from the mid-portion. Bulge shape failure modes in the samples are caused by the outward buckling of the steel tube occurring due to lateral expansion of concrete. On the other hand, it can be stated that the concrete core failure is caused by the crushing of the concrete material, thus causing deterioration in the steel tube. On the other hand, in light of the experimental and numerical evaluations, it has been clearly seen that there is a good matching and agreement between the experimental and computational results. In addition, the model developed in the current study yielded almost similar axial load versus strain (displacement) results. Moreover, as shown in Figure 5a, there is a formation of buckling on the steel tube of the experimentally tested scsc2-2 labeled specimen given in the study of Lin-Hai and Guo-Huang [38]. In Figure 5b, it has been clearly seen that a similar failure mode could be occurred in the specimen analyzed according to the developed FEM model. It can be stated that the failure mode of the specimen simulated from the developed FEM model is strongly reliable and consistent.

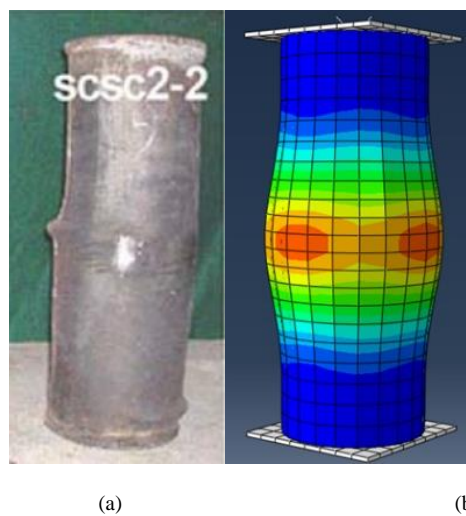


**Figure 5.** Failure mode comparison of scsc2-2 specimen in the study of Lin-Hai and Guo-Huang [38] (a) experimental and (b) FEM results

## V. VERIFICATION OF FINITE ELEMENT MODEL

The previously conducted experimental studies on the CFST circular columns were utilized to confirm the FEA model created in this study [9,15,17,37-62]. The diameter of the column ( $D$ ), the thickness ( $t$ ) and yield strength ( $f_y$ ) of steel tube, the 28-day concrete compressive strength ( $f_c$ ), and the column length ( $L$ ) have been employed as geometric and material properties. The experimental data employed to derive, verify and confirm the model are summarized in Table 1 containing the sources of these datasets.

The FEM design model was established by considering a dataset consisting of a total of 314 experimentally tested CFST circular columns of which properties are presented in Table 1. The properties of these column specimens can be specified as the steel tube outer diameter varying from 60 to 1020 mm, the steel tube thickness ranging from 0.70 to 13.25 mm, the steel tube yield strength ranging from 185 to 853 MPa, and the concrete compressive strength varying between 15 and 130 MPa.

The estimation capability of the developed FEM model containing the designated  $\pm 10\%$  normalization limits is indicated in Figure 6. It obviously indicates that the normalized ultimate axial strength values are well scattered between the designated normalization limit lines. But when the number of normalized ultimate axial strength values falling out of normalization limit lines is compared with that remaining between these lines, it would be overtly seen that the number of normalized ultimate axial strength falling in the normalization limit lines is much more than that falling out of these lines.

**Table 1.** Experimental specimens details and their sources

Reference	Number of Testing Specimens	$D$ (mm)	$t$ (mm)	$L$ (mm)	$f_c$ (MPa)	$f_y$ (MPa)	$N_{u,experimental}$ (kN)
[9]	5	114-168	5.0-8.0	248-330	29-114	365	1876-3101
[15]	8	114-115	3.8-5.0	300-301	26-90	343-365	948-1787
[17]	6	113	2.9	340	20-32	360	730-822
[37]	3	200-300	2.0-5.0	600-900	27-31	266-342	2013-3025
[38]	4	100-200	3.0	300-600	48	304	708-2330
[39]	12	76-153	1.7-4.9	152-305	21-43	363-633	355-2913
[40]	2	150	0.7	480	23-34	248	547-756
[41]	15	165-190	0.9-2.8	578-665	41-108	186-363	1350-3360
[42]	29	102-140	2.4-3.0	305-420	24-130	341-463	676-2175
[43]	36	108-450	2.96-6.5	324-1350	24-82	279-853	941-13776
[44]	10	159-1020	5.1-13.3	447-3060	15-46	291-382	2230-46000
[45]	12	174-179	3.0-9.0	360	21-44	249-283	1220-2730
[46]	6	190	1.2	656-664	95-110	203	2462-3140
[47]	12	297-302	4.5-11.9	891-905	27-79	348-471	3851-9388
[48]	13	101-319	3.0-10.4	304-956	22-50	331-452	649-8289
[49]	28	149-165	1.0-8.0	500	69-73	338-438	1372-3330
[50]	1	120	2.65	360	16	340	640
[51]	36	133-168	3.3-5.4	396-504	34-59	325-392	1140-2480
[52]	26	60-250	1.9-2.0	180-750	70-75	282-404	312-4800
[53]	4	76-114	2.1-3.8	229-343	51	271-358	430-927
[54]	16	108-133	1.0-7.0	378-465	91-101	232-429	1239-3404
[55]	6	165-219	2.7-4.8	510-650	34-62	350	1560-3400
[56]	1	150	3.0	450	60	356	1915
[57]	4	100	1.9	300	112	404	1085-1170
[58]	6	104-114	2.0-6.0	300	31-65	266-412	699-1674
[59]	2	108-150	3.0-4.0	320-330	34-46	274-375	820-1880
[60]	2	300-360	6.0-12.0	720-900	32	479-498	5550-6750
[61]	6	114-167	3.1-5.6	250-350	44-60	300	1042-1873
[62]	3	112-114	1.9-3.7	400	38-47	260-261	667-1011

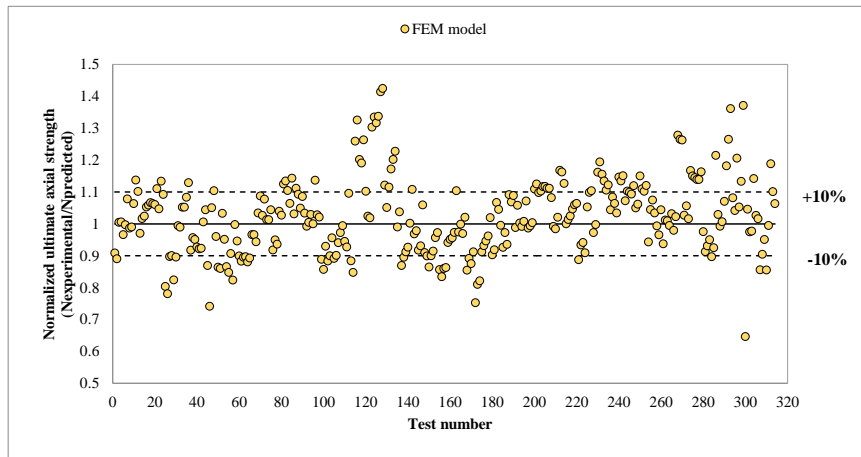


**Figure 6.** The normalized ultimate axial strength-based prediction performance of the developed FEM design model

## VI. COMPARING THE FEM DESIGN MODEL WITH DESIGN CODES

Comparing the effectiveness and prediction capability of the developed FEM design model with the existing design formulations proposed by the design codes and standards was discussed in this part. The peak strength values of the CFST circular columns predicted by the developed FEM design model and the expressions proposed by design codes are compared in Figure 7.

It can be clearly seen that the FEM model proposed in the present study has shown a better estimation capability than many of the code formulae since the load-carrying capacities predicted by the FEM design model have been amassed near the 100% agreement line as demonstrated in Figure 7. A better prediction capability than all others except Eurocode 4 [30] was achieved in the proposed FEM model. But almost similar estimation performance has been observed in the proposed FEM model and the numerical model provided by Eurocode 4 [30].

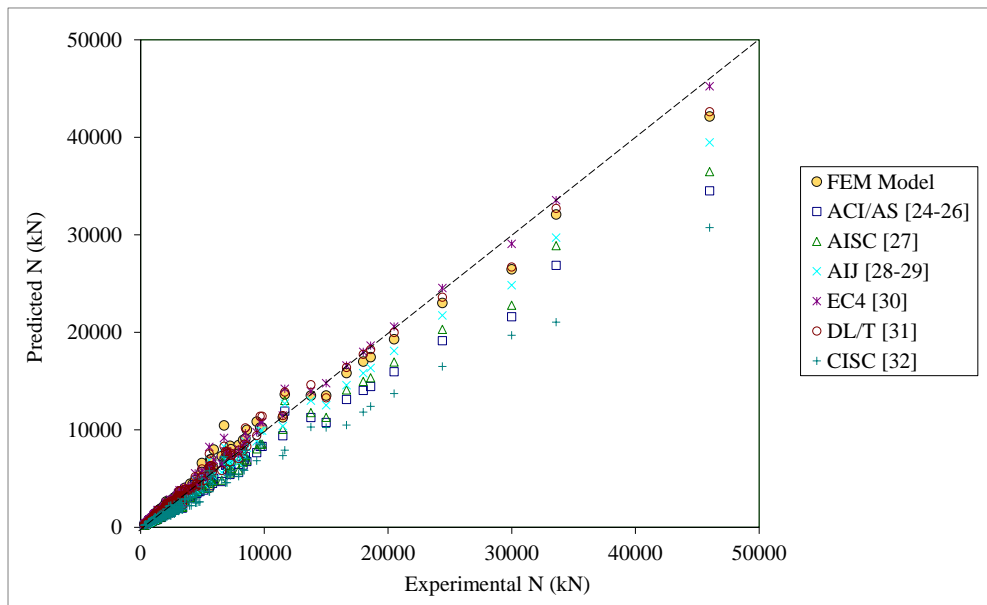


**Figure 7.** Comparing the developed FEM design model with available code design models

The comparison of the normalized ultimate strength values of the developed FEM design model with the empirical models provided by ACI/AS [24-26], AISC [27], AIJ [28,29], Eurocode 4 [30], DL/T [31], and CISC [32] have been shown in Figures 8a-f, respectively. The purpose of presenting the results as graphs is to provide a clearer comparison to comprehend the estimation performance of the FEM model against the code formulas.

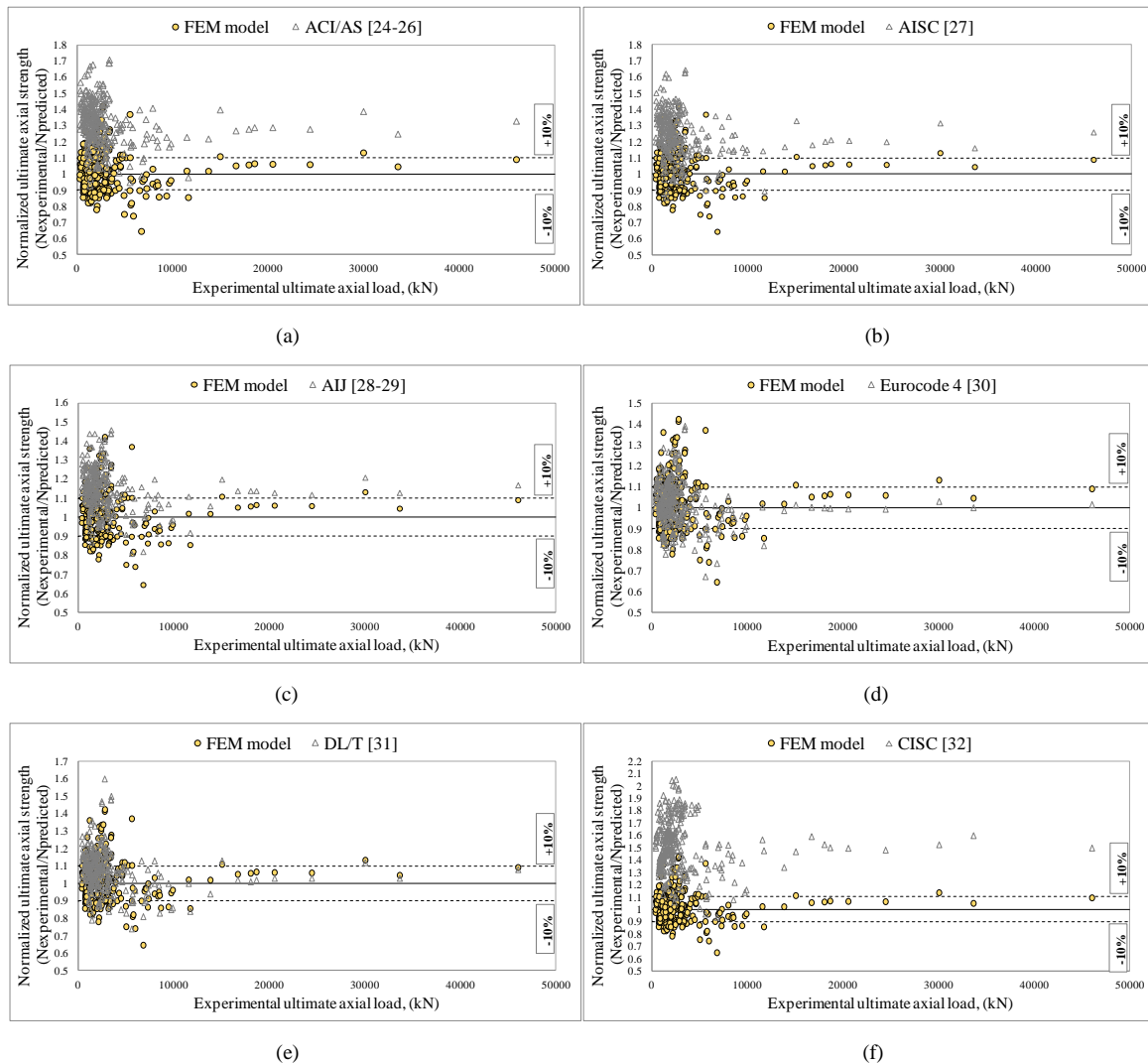


**Figure 8.** Normalized ultimate axial strengths of FEM model and codes formulae vs. experimental ultimate axial loads; (a) ACI/AS, (b) AISC, (c) AIJ, (d) EC4, (e) DL/T, and (f) CISC

Considering the comparison results, it is obviously seen that the FEM model performs better than the empirical models suggested by the codes except for Eurocode 4 [30]. For example, by observing Figures 8a, 8b, 8c, and 8f when the predicted results of the developed FEM design model are measured up against the results estimated by using the empirical models of the ACI/AS [24-26], AISC [27], AIJ [28,29], and CISC [32], respectively, it can be clearly seen that the developed FEM design model has a relatively better estimation capability than the mentioned codes. Because much of the normalized ultimate axial strength values achieved from the FEM model have concentrated between the normalization limits while there are many underestimated ultimate axial strength values obtained by using the empirical models suggested by these codes. Namely, the proposed FEM model and the empirical models provided by the codes have underestimated and overestimated values but the residual ultimate axial strength values of the empirical models of the codes are much greater than that of the proposed FEM model. Moreover, the proposed FEM model has also indicated better performance than the empirical model suggested by the DL/T [31] code, as shown in Figure 8e. But the prediction performance of the DL/T [31] code has been partially better than the other aforementioned four codes. Additionally, according to Figure 8d, it can be forthrightly stated that the Eurocode 4 [30] formula performed approximately similar prediction capability to the proposed FEM model. It has been noticed that the prediction performance of both models is similar, yet, the empirical model of Eurocode 4 [30] is slightly better than the proposed FEM model for some test data.

For a more effective comparison of the FEM model developed in this study and the current design codes, the following statistical parameters have been calculated and presented in Table 2. As observed in Table 2, the lowest MAPE value has been attained from the empirical model suggested by Eurocode 4 [30]. Although the statistical parameters for the FEM model are more than that of the Eurocode 4 [30] formula, it has been exhibited that the FEM model has better than any other design code.

**Table 2.** Statistical parameters of the developed design model as well as existing design codes

Parameters	FEM Model	ACI/AS [24-26]	AISC [27]	AIJ [28, 29]	EC4 [30]	DL/T [31]	CISC [32]
Mean Absolute Percent Error (MAPE)	8.81	23.06	19.21	13.19	7.72	9.54	32.67
Mean Square Error (MSE)	297708	1560635	1046042	512859	144136	230299	3263203
Root Mean Square Error (RMSE)	546	1249	1023	716	380	480	1806

In this regard, for a more detailed examination, Figure 9 shows the average absolute errors for the specific intervals of the experimental and predicted axial load carrying capacity values. For the  $N_u$  values of less than 5000 kN, error values of the FEM model, Architectural Institute of Japan [28-29], Eurocode 4 [30], and Chinese code DL/T [31] are very close. But for higher  $N_u$  values, the developed FEM design model has exhibited better performance than the American Concrete Institute [24], Australian Standards [25-26], American Institute of Steel Construction [27], and Canadian Institute of Steel Construction [32]. However, the highest errors among the design codes for all  $N_u$  values have been determined for the empirical model of the CISC [32] code. The lowest error for the FEM model has been observed for the  $N_u$  values higher than 10000 kN and its value is about 7%. Among the relationships of the existing design codes, Eurocode 4 [30] has generally demonstrated better estimation performance than the others.

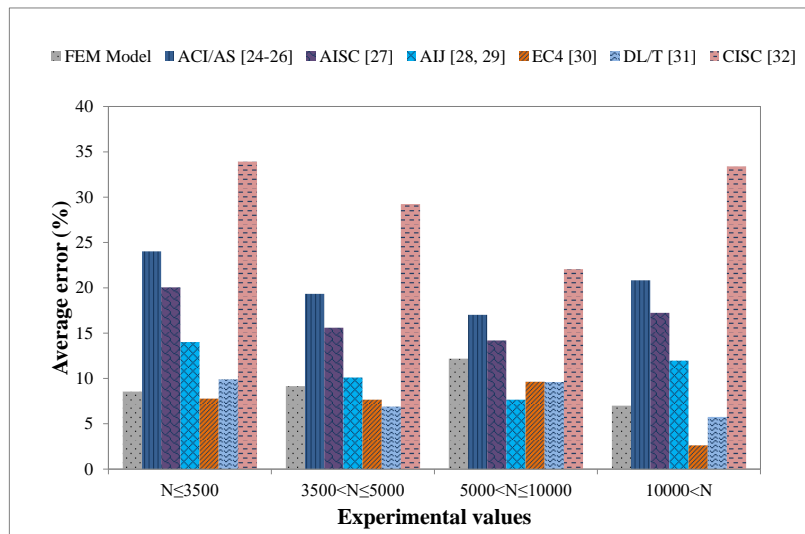


**Figure 9.** Absolute error analysis of the FEM model and design codes according to the axial loads

## VII. CONCLUSIONS

In light of the aforementioned findings and discussions, the following conclusions could be drawn:

- A model for predicting the response of the CFST circular columns was developed using the FEM. The developed design model was confirmed and validated in terms of ultimate axial strength, axial-load displacement response, and failure mechanisms. According to the findings, the developed FEM design model could be employed to estimate the ultimate axial strength of the CFST elliptical column subjected to axial compressive load.
- The FEM design model developed in the current study could be a beneficial tool in the determination of load-displacement response and failure mode of the CFST circular columns.

- The predicted ultimate axial strengths achieved from the developed FEM design model were compared with that estimated using the design models proposed by code/standard. The prediction performance of the developed FEM design model is more consistent and reliable than that of the empirical models provided by the codes/standards except for Eurocode 4. Among these predictive empirical models given in the codes/standards, the best prediction performance has been achieved from the model of Eurocode 4.

- The prediction performance of the developed FEM design model and design formulae proposed by codes/standards were also statistically assessed. The statistical evaluation of the prediction performances demonstrated that the developed FEM design model and the empirical models proposed by AIJ, EC4, and DL/T had very close error values. The proposed FEM design model indicated a better prediction performance than the empirical models proposed by ACI/AS, AISC, and CISC.

- The developed FEM design model predicted not only the ultimate axial strength but also the full load-displacement curves and failure mechanism of such composite members. For this reason, instead of using the aforementioned design models proposed by codes/standards to predict the performance of CFST columns, employing a FEM-based design model confirmed and validated by experimental results in characterizing the behavior of such composite members will be more reliable and functional.

#### REFERENCES

- [1] Tsuda, K., Matsui, C., & Ishibashi, Y. (1995). Stability design of slender concrete filled steel tubular columns. In: Proc. of the Fifth Asia-Pacific Conference on Structural Engineering and Construction (EASEC-5), 439-444.
- [2] Zeghiche, J., & Chaoui, K. (2005). An experimental behaviour of concrete-filled steel tubular columns. *Journal of Constructional Steel Research*, 61, 53-66.
- [3] Lu, Z.H., & Zhao, Y.G. (2010). Suggested empirical models for the axial capacity of circular CFT stub column. *Journal of Constructional Steel Research*, 66, 850-862.
- [4] Han, L.H., Li, W., & Bjorhovde, R. (2014). Developments and advanced applications of concrete-filled steel tubular (CFST) structures: Members. *Journal of Constructional Steel Research*, 100, 211-228.
- [5] Li, N., Lu, Y.Y., Li, S., & Liang, H.J. (2015). Statistical-based evaluation of design codes for circular concrete-filled steel tube columns. *Steel and Composite Structure*, 18, 519-546.
- [6] Zhao, X.L., & Han, L.H. (2006). Double skin composite construction. *Progress in Structural Engineering and Materials*, 8, 93-102.
- [7] Roeder, C.W., Lehman, D.E., & Bishop, E. (2010). Strength and stiffness of circular concrete-filled tubes. *Journal of Structural Engineering*, 136, 1545-1553.
- [8] Lu, Z.H., & Zhao, Y.G. (2010). Suggested empirical models for the axial capacity of circular CFT stub column. *Journal of Constructional Steel Research*, 66, 850-862.
- [9] Ho, J.C.M., & Lai, M.H. (2013). Behaviour of uni-axially loaded CFST columns connected by tie bars. *Journal of Constructional Steel Research*, 83, 37-50.
- [10] D'Aniello, M., Güneyisi, E.M., Landolfo, R., & Mermerdaş, K. (2014). Analytical prediction of available rotation capacity of cold-formed rectangular and square hollow section beams. *Thin-Walled Structures*, 77, 141-152.
- [11] Güneyisi, E.M., Gültekin, A., & Mermerdaş, K. (2016). Ultimate capacity prediction of axially loaded CFST short columns. *International Journal of Steel Structures*, 16, 99-104.
- [12] İpek, S., & Güneyisi, E.M. (2019). Ultimate axial strength of concrete-filled double skin steel tubular column sections. *Advances in Civil Engineering*, 11, 1-19.
- [13] Güneyisi, E.M., & Nour, A.I. (2019). Axial compression capacity of circular CFST columns transversely strengthened by FRP. *Engineering Structures*, 191, 417-431.
- [14] Furlong, R.W. (1967). Strength of steel-encased concrete beam-columns. *Journal of the Structural Division (ASCE)*, 93, 113-124.

- [15] Giakoumelis, G., & Lam, D. (2004). Axial capacity of circular concrete-filled tube columns. *Journal of Constructional Steel Research*, 60, 1049-1068.
- [16] Rao, S.S. (2004). *The finite element method in engineering* (4<sup>th</sup> Ed). Butterworth-Heinemann.
- [17] Gupta, P.K., Sarda, S.M., & Kumar, M.S. (2007). Experimental and computational study of concrete filled steel tubular columns under axial loads. *Journal of Constructional Steel Research*, 63, 182-193.
- [18] Dai, X., & Lam, D. (2010). Numerical modelling of the axial compressive behaviour of short concrete-filled elliptical steel columns. *Journal of Constructional Steel Research*, 66, 931-942.
- [19] El-Heweity, M.M. (2012). On the performance of circular concrete-filled high-strength steel columns under axial loading. *Alexandria Engineering Journal*, 51, 109-119.
- [20] Wang, R., Han, L.H., & Hou, C.C. (2013). The behavior of concrete filled steel tubular (CFST) members under lateral impact: Experiment and FEA model. *Journal of Constructional Steel Research*, 80, 188-201.
- [21] Al-Ani, Y.R. (2018). Finite element study to address the axial capacity of the circular concrete filled steel tubular stub columns. *Thin-Walled Structures*, 126, 2-15.
- [22] Ellobody, E., Young, B., & Lam, D. (2006). Behaviour of normal and high strength concrete-filled compact steel tube circular stub columns. *Journal of Constructional Steel Research*, 62, 706-715.
- [23] ABAQUS. (2014). *Analysis user's manuals and example problems manuals*. Dassault Systemes Simulia Corp, Providence, RI, USA.
- [24] ACI318-05. (2005). *Building code requirements for structural concrete (ACI 318-05) and commentary (ACI 318R-05)*. Farmington Hills (MI, USA): American Concrete Institute.
- [25] AS4100. (1998). *Steel structures*. Sydney (Australia): Standards Association of Australia.
- [26] AS3600. (2001). *Concrete structures*. Sydney (Australia): Standards Association of Australia; 2001.
- [27] AISC. (2005). *Load and resistance factor design (LRFD) specification for structural steel buildings*. Chicago (IL, USA): American Institute of Steel Construction.
- [28] AIJ. (1997). *Recommendations for design and construction of concrete filled steel tubular structures*. Tokyo (Japan): Architectural Institute of Japan.
- [29] AIJ. (2001). *Standards for structural calculation of steel reinforced concrete structures 5th ed*. Tokyo (Japan): Architectural Institute of Japan.
- [30] EN 1994. (2004). *Design of composite steel and concrete structures – Eurocode 4: Part 1.1, General rules and rules for buildings*. European Committee for Standardization: British Standards Institution.
- [31] DL/T 5085. (1999). *Chinese design code for steel-concrete composite structures*. Beijing (China): Chinese Electricity Press.
- [32] CISC. (1997). *Canadian Institute of Steel Construction, Handbook of Steel Construction*, 7<sup>th</sup> Ed. ISBN 0-88811-088-X, Ontario.
- [33] Han, L.H., & Huo, J.S. (2003). Concrete-filled HSS columns after exposure to ISO-834 standard fire. *Journal of Structural Engineering*, 129, 68-78.
- [34] Hu, H.T., Huang, C.H., Wu, M.H., & Wu, Y.M. (2003). Nonlinear analysis of axially loaded concrete-filled tube columns with confinement effect. *Journal of Structural Engineering*, 129(10), 1322-1329
- [35] Binici, B. (2005). An analytical model for stress-strain behavior of confined concrete. *Engineering Structures*, 27(7), 1040-1051.
- [36] İpek, S., Erdoğan, A., & Güneyisi E.M. (2021). Compressive behavior of concrete-filled double skin steel tubular short columns with the elliptical hollow section. *Journal of Building Engineering*, 38, 102200.
- [37] Huang, C.S., Yeh, Y.K., Liu, G.Y., Hu, H.T., Tsai, K.C., Weng, Y.T., Wang, S.H., & Wu, M.H. (2002). Axial load behavior of stiffened concrete-filled steel columns. *Journal of Structural Engineering*, 128, 1222-1230.

- [38] Lin-Hai, H., & Guo-Huang, Y. (2004). Experimental behaviour of thin-walled hollow structural steel (HSS) columns filled with self-consolidating concrete (SCC). *Thin-Walled Structures*, 42, 1357-1377.
- [39] Gardner, N.J., & Jacobson, E.R. (1967). Structural behavior of concrete-filled steel tubes. *ACI Structural Journal*, 64, 404-412.
- [40] Lin, C.Y. (1988). Axial capacity of concrete infilled cold-formed steel columns. In: The Ninth International Specialty Conference on Cold-Formed Steel Structures, November 8-9, St Louis, Missouri, USA, 443-457.
- [41] O'Shea, M.D., & Bridge, R.Q. (2000). Design of circular thin-walled concrete filled steel tubes. *Journal of Structural Engineering*, 126(11), 1295-1303.
- [42] Saisho, M., Abe, T., & Nakaya, K. (1999). Ultimate bending strength of high-strength concrete filled steel tube column. *Journal of Structural and Construction Engineering*, 523, 133-140.
- [43] Sakino, K., Nakahara, H., Morino, S., & Nishiyama, I. (2004). Behavior of centrally loaded concrete-filled steel-tube short columns. *Journal of Structural Engineering*, 130, 180-188.
- [44] Luksha, L.K., & Nesterovich, A.P. (1991). Strength testing of larger-diameter concrete filled steel tubular members. In: The 3rd International Conference on Steel-concrete Composite Structures, September 26-29, Fukuoka, Japan, 67-70.
- [45] Sakino, K., & Hayashi, H. (1991). Behavior of concrete filled steel tubular stub columns under concentric loading. In: The 3rd International Conference on Steel-concrete Composite Structures, September 26-29, Fukuoka, Japan, 25-30.
- [46] O'Shea, M.D., & Bridge, R.Q. (1994). Tests of thin-walled concrete-filled steel tubes. In: The Twelfth International Specialty Conference on Cold-Formed Steel Structures; October 18-19, St. Louis, Missouri, USA, 399-419.
- [47] Kato, B. (1995). Compressive strength and deformation capacity of concrete-filled tubular stub columns (Strength and rotation capacity of concrete-filled tubular columns, Part 1). *Journal of Structural and Construction Engineering*, 468, 183-191.
- [48] Yamamoto, T., Kawaguchi, J., & Morino, S. (2002). Experimental study of the size effect on the behaviour of concrete filled circular steel tube columns under axial compression. *Journal of Structural and Construction Engineering*, 561, 237-244.
- [49] Yu, Z., Ding, F., & Lin, S. (2002). Researches on behavior of high-performance concrete filled tubular steel short columns. *Journal of Building Engineering*, 23, 41-47.
- [50] Han, L.H., & Yao, G.H. (2003). Behaviour of concrete-filled hollow structural steel (HSS) columns with pre-load on the steel tubes. *Journal of Constructional Steel Research*, 59, 1455-1475.
- [51] Zhang, S., & Wang, Y. (2004). Failure modes of short columns of high-strength concrete filled steel tubes. *China Civil Engineering Journal*, 37, 1-10.
- [52] Han, L.H., Yao, G.F., & Zhao, X.L. (2005). Experiment behavior of thin-walled hollow structural steel (HSS) stub columns filled with self-consolidating concrete (SCC). *Journal of Constructional Steel Research*, 61, 124-169.
- [53] Kang, H.S., Lim, S.H., Moon, T.S., & Stiemer, S.F. (2005). Experimental study on the behavior of CFT stub columns filled with PCC subject to concentric compressive loads. *Steel and Composite Structures*, 5, 17-34.
- [54] Tan, K. (2006). Analysis of formulae for calculating loading bearing capacity of steel tubular high strength concrete. *Journal of Southwest University of Science and Technology*, 21, 7-10.
- [55] Yu, Z.W., Ding, F.X., & Cai, C.S. (2007). Experimental behavior of circular concrete-filled steel tube stub columns. *Journal of Constructional Steel Research*, 63, 165-174.
- [56] Tao, Z., Han, L.H., & Wang, L.L. (2007). Compressive and flexural behaviour of CFRP-repaired concrete-filled steel tubes after exposure to fire. *Journal of Constructional Steel Research*, 63, 1116-1126.
- [57] Yu, Q., Tao, Z., & Wu, Y.X. (2008). Experimental behaviour of high performance concrete-filled steel tubular columns. *Thin-Walled Structures*, 46, 362-370.

- [58] Lam, D., & Gardner, L. (2008). Structural design of stainless steel concrete filled columns. *Journal of Constructional Steel Research*, 64, 1275-1282.
- [59] Huo, J., Huang, G., & Xiao, Y. (2009). Effects of sustained axial load and cooling phase on post-fire behaviour of concrete-filled steel tubular stub columns. *Journal of Constructional Steel Research*, 65, 1664-1676.
- [60] Lee, S.H., Uy, B., Kim, S.H., Choi, Y.H., & Choi, S.M. (2001). Behavior of high-strength circular concrete-filled steel tubular (CFST) column under eccentric loading. *Journal of Constructional Steel Research*, 67, 1-13.
- [61] Abed, F., Al Hamaydeh, M., & Abdalla, S. (2013). Experimental and numerical investigations of the compressive behavior of concrete filled steel tubes (CFSTs). *Journal of Constructional Steel Research*, 80, 429-439.
- [62] Chang, X., Fu, L., Zhao, H.B., & Zhang, Y.B. (2013). Behaviors of axially loaded circular concrete-filled steel tube (CFT) stub columns with notch in steel tubes. *Thin-Walled Structures*, 73, 273-280.